Accessibility-Based Clustering for Efficient Learning of Locomotion Skills

Chong Zhang[1]*, Wanming Yu[2]*, and Zhibin Li[2]†

***Abstract*— For model-free deep reinforcement learning of quadruped locomotion, the initialization of robot configurations is crucial for data efficiency and robustness. This work focuses on algorithmic improvements of data efficiency and robustness simultaneously through automatic discovery of initial states, which is achieved by our proposed K-Access algorithm based on accessibility metrics. Specifically, we formulated accessibility metrics to measure the difficulty of transitions between two arbitrary states, and proposed a novel K-Access algorithm for state-space clustering that automatically discovers the centroids of the static-pose clusters based on the accessibility metrics. By using the discovered centroidal static poses as the initial states, we can improve data efficiency by reducing redundant explorations, and enhance the robustness by more effective explorations from the centroids to sampled poses. Focusing on fall recovery as a very hard set of locomotion skills, we validated our method extensively using an 8-DoF quadrupedal robot *Bittle*. Compared to the baselines, the learning curve of our method converges much faster, requiring only 60% of training episodes. With our method, the robot can successfully recover to standing poses within 3 seconds in 99.4% of the test cases. Moreover, the method can generalize to other difficult skills successfully, such as backflipping.**

I. Introduction

Among robot locomotion skills, trotting and some other tasks are easy in terms of exploration, while fall recovery is difficult due to many possible robot states. The ability to recover from a fall is critical for legged robots to improve their robustness against potential failures.

For fall recovery, manually-designed joint trajectories [1] are laborious, and their robustness in different environments is not guaranteed. Optimization-based [2] methods require a significant amount of time to obtain a feasible solution since dynamic models and complex contact situations need to be considered [3]. Therefore, optimization approaches are difficult to achieve real-time fall recovery. To overcome the limitations of these methods, model-free deep reinforcement learning (DRL) methods [4] serve as a promising alternative for generating diverse locomotion behaviors, such as fall recovery.

However, learning fall recovery via DRL suffers from hard exploration, i.e., to explore in domains with sparse, delayed, or deceptive rewards, and redundant exploration, i.e., certain regions of the state space being too frequently visited while training because of skewed data collection. Both hard exploration and redundant exploration can affect the data efficiency and learning performance. Initial state distribution is one of the key factors that affect the efficiency of exploration. Figure 1 illustrates some cases of initial state distributions regarding their levels of redundant exploration and hard exploration. To increase the data efficiency, both redundant exploration and hard exploration should be reduced.

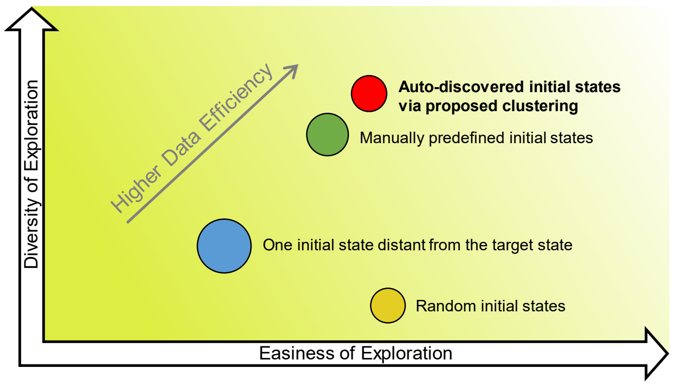
Diversity of Exploration
Easiness of Exploration
Higher Data Efficiency
Auto-discovered initial states via proposed clustering
Manually predefined initial states
One initial state distant from the target state
Random initial states

Fig. 1. Levels of redundant explorations and hard exploration across different initial state distributions. Higher redundancy means lower diversity of exploration. Our proposed automatic discovery of initial states via clustering is more data efficient.

Currently, there are 3 common ways to design initial state distributions for learning fall recovery via DRL: 1) initialization from demonstrations [5], 2) initialization from random distributions [6], and 3) initialization from predefined poses [4]. For initialization from demonstrations, the performance is limited to the demonstrated examples. For initialization from random distributions, it is not data efficient [6] because of the redundant exploration. Also, corner cases may suffer from insufficient exploration because of skewed data collection. As a result, the diversity of exploration cannot be guaranteed. For initialization from predefined poses, states that lack intuition or heuristics are very likely to be missed, and the generalization can be a problem despite high data efficiency.

In this work, we aim to automatically discover initial states that can help achieve high robustness while still being data efficient. We propose to achieve this by clustering the static poses of the robot and applying centroids as initial states.

A. Related Work

Regarding DRL, model-free DRL has been a commonly-used method for fall recovery and other locomotion tasks [7] [8]. In contrast to model-based methods such as model predictive control [9] [10], trajectory optimization [11] [12]

*These authors contributed equally to this work.

†Corresponding author. Email: zhibin.li@ed.ac.uk

[1]Chong Zhang is with Department of Precision Instrument, Tsinghua University, Beijing, 100084 China.
Email: chong-zh18@mails.tsinghua.edu.cn

[2]Wanming Yu and Zhibin Li are with the School of Informatics, University of Edinburgh, 10 Crichton St, Edinburgh EH8 9AB, United Kingdom.
Email: wanming.yu@ed.ac.uk, zhibin.li@ed.ac.uk

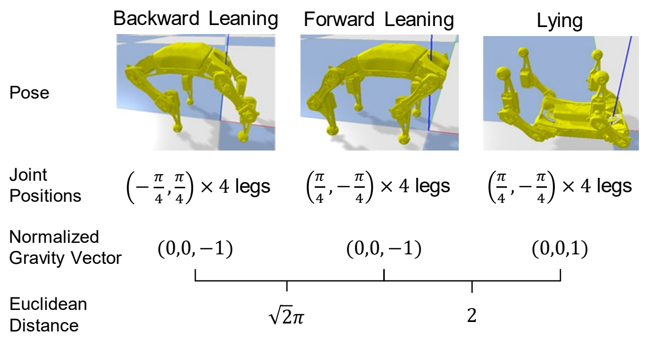

Backward Leaning
Forward Leaning
Lying
Pose
Joint Positions
$\left(-\frac{\pi}{4},\frac{\pi}{4}\right)\times 4$ legs
$\left(\frac{\pi}{4},-\frac{\pi}{4}\right)\times 4$ legs
$\left(\frac{\pi}{4},-\frac{\pi}{4}\right)\times 4$ legs
Normalized Gravity Vector
$(0,0,-1)$
$(0,0,-1)$
$(0,0,1)$
Euclidean Distance
$\sqrt{2}\pi$
2

Fig. 2. An erroneous case of using Euclidean distance metric. The distance between a backward leaning stance and a forward leaning stance should be smaller than that between a forward leaning stance and a lying pose.

and Bayesian optimization [13], model-free methods do not require explicit knowledge of complex dynamics, and support fast online computation without mathematical optimization. The most popular model-free DRL algorithms for robot locomotion are the proximal policy optimization (PPO) algorithm [14] and the soft actor-critic (SAC) algorithm [15]. Besides, the training of DRL can be greatly expedited by GPU-based parallelization [16].

Regarding clustering, common clustering methods have successful applications in RL, such as value function approximation [17], but they fail to achieve ideal clustering of diverse robot states. For centroid-based methods such as K-Means [18] and density-based methods such as DBSCAN [19], the problem is the metric for clustering, which will be discussed later. For pattern-based methods [20], state transitions of the robot can be regarded as edges in a directed graph. However, the existing methods could not achieve the desired clustering effect of robot states as well, which will be discussed in I-B.

Regarding the metric, we usually adopt the Euclidean distance assuming that all dimensions are orthogonal, i.e., the coordinates are based on the unit orthogonal basis, and that the distances are undirected, i.e., $\|x-y\|_2 = \|y-x\|_2$. However, both the orthogonality and the undirected distances are problematic for robot poses. For the state space of static poses, we tend to use the combination of the normalized gravity vector and the joint positions [4], and these feature dimensions are not orthogonal. Also, it is difficult to determine the scale of the features. A failure case of the Euclidean distance is shown in Fig. 2. The undirected distances are also inapplicable because the robot's transitions are directed. For instance, it is easy to fall from a standing pose to a lying pose, but difficult to recover from a lying pose to a standing pose.

There are also some metric learning methods, but they are time-consuming and difficult to obtain values for each start-end pose pair. In [21], the distance metric is approximated for state-space rapidly-exploring random trees (RRTs) [22], but it is impractical to construct an RRT for each pose. In [23], the metric is learned during the training process, but we do not want to learn the metric for a certain DRL model before clustering.

B. *Motivation and Our Contribution*

In this paper, we aim to find the initial states that can help reduce hard exploration and redundant exploration during the training process to learn robust fall recovery efficiently. To ensure robustness, the initial states need to cover as much of the state space as possible. We expect the centroids of the static-pose clusters to serve as the ideal initial states.

In terms of the metric for clustering, we propose the accessibility metric in II-A to overcome the shortcomings of the Euclidean distance mentioned in I-A.

For pattern-based clustering, we tried the directed Louvain method [24], the Infomap method [25], and the spectral clustering method [26]. The directed Louvain method failed because it cannot properly distinguish the direction of the edges (state transitions in this paper) [27]. The Infomap method failed because unreachable states could exist in the same cluster, which means that the model was expected to explore states that can hardly be reached from the initial states. The spectral clustering method failed because the number of clusters was too small, which indicates low robustness. To obtain the ideal clustering effect, we propose a new accessibility-based clustering method called K-Access in II-C.

Our contributions in this paper include:

- An accessibility metric to quantify the level of difficulties for a robot to transition from one physical state/configuration to another;
- A K-Access algorithm based on the accessibility metric, for state-space clustering, which is adapted from the K-Means++ algorithm;
- A pipeline of automatically discovering feasible initial states, based on their inter-connected transitions, for efficient learning of robot fall recovery and other tasks.

With our proposed method, the data efficiency of DRL models can be greatly improved by avoiding repeated and redundant explorations, and the robustness can be greatly enhanced because of the wide range of searched states and their explored inter-connections.

II. Methodology

In this section, the concept of accessibility is firstly introduced in II-A. The criteria of good initial state distributions are discussed in II-B, and the K-Access algorithm is presented in II-C. In II-D, the DRL is applied to the learning of fall recovery, and the entire pipeline is shown in Fig. 5. We also provide generic principles to apply our proposed method to other tasks in II-E.

A. *Accessibility*

To model the difficulty of transitions from one state to another, we propose the accessibility metric. Figure 3 demonstrates the concept of accessibility. Consider an initial state s_0 in the state space S. There is a region $R \subseteq S$ that can be easily and effectively explored from s_0, and this region can be mathematically defined as

$$R = \{s | s \in S, t(s_0, s) < t_0\}, \tag{1}$$

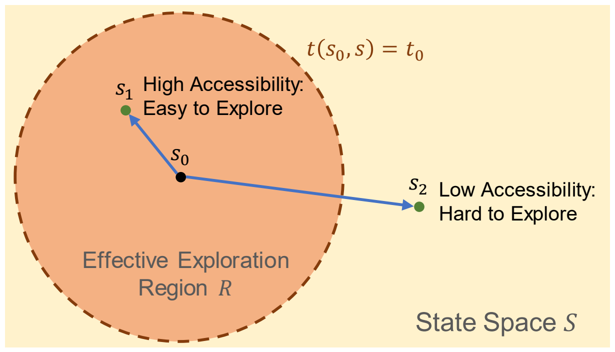
$t(s_0, s) = t_0$
s_1 High Accessibility: Easy to Explore
s_0
s_2 Low Accessibility: Hard to Explore
Effective Exploration Region R
State Space S

Fig. 3. An illustration of accessibility. The accessibility value corresponds to the difficulty of a state being explored from the initial state.

where $t(s_0, s)$ is the minimal time cost (in seconds) of the transition from s_0 to s, and t_0 is a positive value. R is called the effective exploration region of s_0.

Consider another two states $s_1 \in R$ and $s_2 \notin R$. We can say that the accessibility from s_0 to s_1 is high, and it is easy to explore s_1 from s_0. In contrast, the accessibility from s_0 to s_2 is low, and it is difficult to explore s_2 from s_0.

Mathematically, we define the accessibility from $s_i \in S$ to $s_j \in S$ as

$$\text{access}(s_i, s_j) = e^{-t(s_i, s_j)}. \tag{2}$$

In practice, it is difficult to get the minimal time cost $t(s_i, s_j)$, and we approximate it by the response time of direct PD control that changes the joint positions from s_i to those of s_j. The response time is infinity if the final state is not s_j. The range of accessibility is

$$\text{access}(s_i, s_j) \in [0, 1]. \tag{3}$$

If the accessibility is zero, s_j is unreachable from s_i. If the accessibility is one, $s_i = s_j$.

B. What Makes Good Initial States

With the concept of accessibility, we can evaluate whether a distribution of initial states is good for the DRL exploration. Figure 4 shows different cases of initial state distributions. For data efficiency, redundant exploration and hard exploration are detrimental. For robustness, the effective exploration regions should cover as much state space as possible. For the trade-off between data efficiency and robustness, we need to select the initial states and their effective exploration regions with sufficient coverage but minimal redundancy.

To ensure enough coverage, we propose to randomly sample a wide range of static poses. Then we cluster the sampled poses to reduce the redundancy. We expect that the centroids of the obtained clusters can make good initial states. Their effective exploration regions should cover most of the state space, and there should be little overlapping.

Based on the discussion above, we can evaluate whether the obtained clusters are good. If the inter-cluster accessibility is too high, there is much overlapping since the centroids can be too close to each other, and the data efficiency is decreased due to redundant exploration. If the intra-cluster accessibility is too low, the coverage is low since many

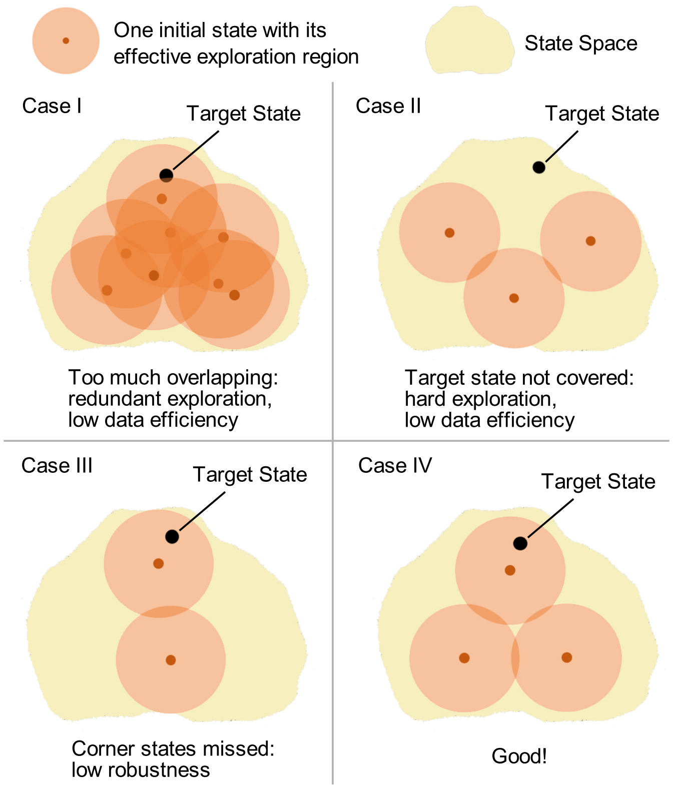
One initial state with its effective exploration region
State Space
Case I
Target State
Too much overlapping: redundant exploration, low data efficiency
Case II
Target State
Target state not covered: hard exploration, low data efficiency
Case III
Target State
Corner states missed: low robustness
Case IV
Target State
Good!

Fig. 4. Different cases of initial state distributions. The target state is what the agent is expected to achieve during exploration. It represents certain states for certain tasks (see II-E). Too much overlapping of the effective exploration regions results in redundant exploration and decreased data efficiency. For easy exploration and robustness, high coverage of the regions is required. Randomized initialization corresponds to case I, and we expect the auto-discovered initial states are similar to case IV.

samples are not in the effective exploration region of their centroids, and there can be poses that are difficult to explore from the centroids. Hence, for good clustering results, the inter-cluster accessibility should be low, and the intra-cluster accessibility should be high.

C. K-Access Algorithm

Based on the accessibility metric proposed in II-A, we refer to the K-means++ algorithm [28] and propose the K-Access clustering method. The algorithm is presented in Algorithm 1. The inputs are the number of clusters k and the accessibility matrix A for the sampled states $s_0, s_1, \ldots, s_{n-1} \in S$. The shape of A is (n,n), and $A[i,j]$ is the accessibility from s_i to s_j $(i, j \in \{0, \ldots, n-1\})$. The outputs are the indices of the centroids $cIndex = (c_0, \ldots, c_{k-1})$ and the centroids of each state's cluster $assignment = (a_0, \ldots, a_{n-1})$.

Similar to the K-Means++ algorithm, the first step of K-Access algorithm is to initialize the centroids, and then we repeat the assignment step and the update step until the assignments no longer change, as described below.

1) Initialization of centroids: The first centroid is randomly selected (line 2), and each new centroid is the sample which is the furthest from the already selected centroids (line 3-6).
2) Assignment of samples to clusters: Each sample state is assigned to the cluster of which the centroid has the

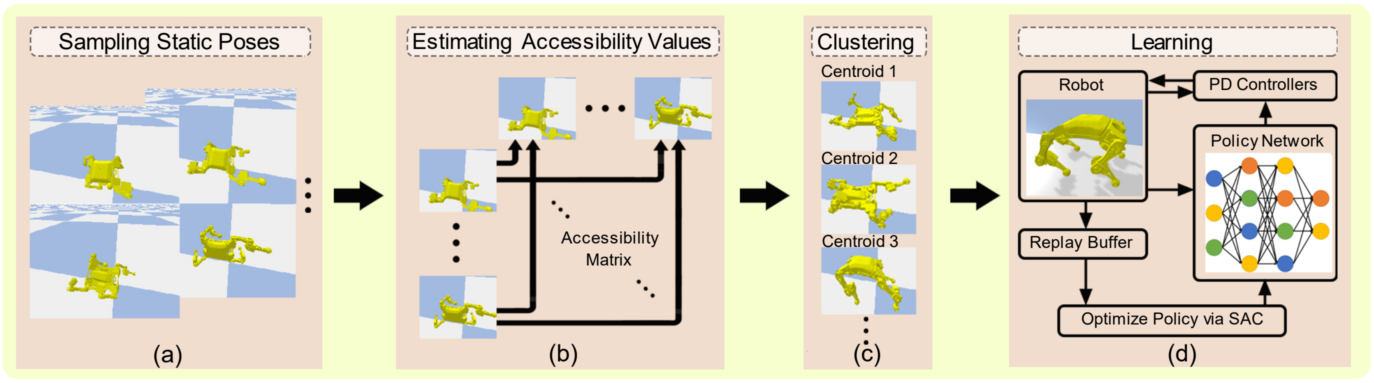

Fig. 5. Pipeline of the proposed method. First, static poses are randomly sampled. Second, the estimated accessibility values are obtained via simulation. Third, the proposed K-Access algorithm selects and discovers the optimal initial states. Finally, the DRL agent learns fall recovery through exploration based on the discovered initial states.

Algorithm 1 K-Access(k, A)

```
1:  $cIndex \leftarrow \text{zeros}(k)$;                          ◁ indices of centroids
2:  $cIndex[0] \leftarrow \text{randInt}(0, k)$;
3:  for $i = 1$ to $k-1$ do
4:      $CAccess \leftarrow \sum_{j=0}^{i-1} (A[cIndex[j], :] + A[:, cIndex[j]])$;
5:      $cIndex[i] \leftarrow \arg\min_{j} CAccess[j]$;  ◁ initialize $cIndex$
6:  end for
7:  $assignment[i] \leftarrow \arg\max_{c \in cIndex} A[c, i], \forall i < n, i \in \mathbb{N}$;
8:  $preassign \leftarrow \text{zeros}(n)$;                  ◁ previous $assignment$
9:  while $preassign \neq assignment$ do
10:     $preassign \leftarrow assignment$;
11:     $cIndex[i] \leftarrow \arg\max_{j \text{ s.t. } a_j = c_i} \min_{a_l = c_i} A[j, l], \forall i < k, i \in \mathbb{N}$;
12:     $assignment[i] \leftarrow \arg\max_{c \in cIndex} A[c, i], \forall i < n, i \in \mathbb{N}$;
13: end while
14: return $cIndex, assignment$
```

highest accessibility to this state (line 7,12). Note that we only consider the accessibility of single direction here.

3) Update of the choice of centroids: The new centroid has the maximal neighborhood accessibility, and the neighborhood accessibility of one state is represented by the minimal accessibility value from the state to its neighbors in the same cluster (line 11). To ensure robustness, we do not take the average, which differs from K-Means++.

Finally, the K-Access algorithm can converge to a result that prefers high intra-cluster accessibility and low inter-cluster accessibility. To determine the number of clusters, we propose an index based on the discussions in II-B that good clustering results should have high intra-cluster accessibility and low inter-cluster accessibility. The index I is defined as

$$I = \overline{\log(A_{\text{intra}})} - \overline{\log(A_{\text{inter}})} - \alpha \cdot |\Lambda|, \tag{4}$$

where A_{intra} is the intra-cluster accessibility array of size k, A_{inter} is the inter-cluster accessibility of size (k, k), and $\alpha \cdot |\Lambda|$ is the regularization term. The clustering results are better if the index is larger, and the inter/intra-cluster metrics are also defined in a different way from K-Means++. To be specific, in our implementation,

$$A_{\text{intra}}[i] = \min_{a_j = c_i} A[c_i, j], \forall i < k, \tag{5}$$

$$A_{\text{inter}}[i, j] = \begin{cases} \underset{a_l = c_i}{\text{mean}}\, A[a_l, c_j], \forall i \neq j, \\ 1, \forall i = j, \end{cases} \tag{6}$$

where $i < k, i \in \mathbb{N}, j < k, j \in \mathbb{N}$,

$$\Lambda = \left\{ c_i \mid i < k, i \in \mathbb{N}, |\{ j \mid a_j = c_i, j < n, j \in \mathbb{N} \}| = 1 \right\}, \tag{7}$$

and α is a real value (recommended value: 1). We penalize the number of one-sample clusters because such clusters can hardly be hit and they may exist because of extreme coincidences. In most cases, one-sample clusters are also accessible from other clusters. Therefore, one-sample clusters should be rare or non-existent, otherwise the training process may suffer from unnecessary or redundant experiences.

In Fig. 5, the K-Access algorithm is applied in (c), after the static poses are sampled in (a) and the accessibility values are estimated in (b).

D. *Fall Recovery Learning*

Our DRL framework is shown in Fig. 6. The state space consists of the orientation (represented by the normalized gravity vector), the angular velocity of the body, and the joint positions. Here we adopt the positional control according to [29]. The outputs of the policy network are the target joint positions which update at 25 Hz. The PD controllers generate torques based on the target joint positions and the measured joint positions at 300 Hz. The SAC algorithm is applied for learning. In our implementation, we use the 8-DoF quadrupedal robot Bittle [30] and the PyBullet [31] simulation environment.

The Bittle is equipped with an IMU on its body. The angular velocity can be directly accessed from the IMU. The orientation is represented as the gravity vector in the body frame which is normalized to be of length 1. The gravity vector can be computed using the IMU measurements.

The reward function is the sum of reward terms in Table I. The *jump* regularization term aims to penalize the robot for actions (e.g., backflipping) to adjust the orientation in the air, and the action difference term serves to reduce

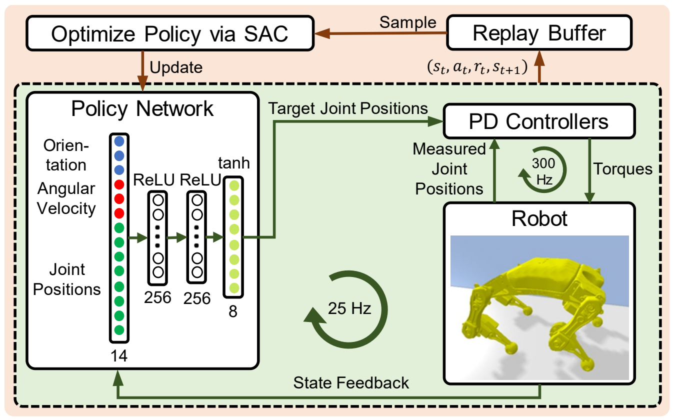

Fig. 6. DRL framework overview. The policy network generates the target joint positions at 25 Hz. The actuators follow the 300 Hz impedance control based on the target and the measured joint positions. The SAC algorithm is applied for learning the feedback control policy.

TABLE I
REWARD TERMS FOR DRL.

Symbols	
h	body height
g_{ori}	normalized gravity vector
Ω	body angular velocity
τ	vector of joint torques
ω	vector of joint velocity
c_{b}	0 if the body touches the ground, otherwise 1
c_{f}	0.3×the number of feet that touch the ground
h_{f}	vector of the distances from four feet to the ground
d_{s}	the shortest distance from the robot to the ground
p	vector of the measured joint positions
p^{t}	vector of the target joint positions
$\hat{\cdot}$	target value
Reward Terms	
Height	$0.667 \times \text{RBF}(h, \hat{h}, -2000)$
Orientation	$0.333 \times \text{RBF}(g_{\text{ori}}, [0,0,-1]^T, -5)$
Angular velocity	$0.067 \times \text{RBF}(\Omega, 0, -0.05)$
Joint torques	$0.067 \times \text{RBF}(\tau, 0, -5)$
Joint velocity	$0.067 \times \text{RBF}(\omega, 0, -0.05)$
Contact	$0.067 \times c_{\text{b}} + 0.033 \times c_{\text{f}}$
Foot lift	$0.067 \times \text{RBF}(h_{\text{f}}, 0, -100)$
Jump regularization	$0.033 \times \text{RBF}(d_{\text{s}}, 0, -100)$
Action difference	$0.033 \times \text{RBF}(p^{\text{t}}, p, -1)$

unrealistic large movements. We assign larger weights to the reward terms related to body height and orientation since we characterize a standing pose mainly by the body height and the orientation for the fall recovery task. The radial basis function (RBF) applied in these terms is defined as:

$$\text{RBF}(x, y, \alpha) = \exp\left(\alpha \cdot \|x - y\|_2^2\right). \tag{8}$$

The learning process is the last stage (d) of the pipeline in Fig. 5, where we apply the centroids in (c) as the initial states for DRL of quadruped fall recovery.

E. Learning Other Tasks

The proposed method is not limited to fall recovery learning. In III-E, we also validated our method in back-flip learning. The generic principles to apply the proposed method are:

1) Perform clustering in a subspace with feasible and necessary dimensions;
2) Ensure that the target state has the maximum state value $V(s)$ in the subspace;
3) Estimate the accessibility values with time-accuracy trade-off.

The first principle is about how we define the subspace for clustering. The clustering methods tend to suffer in high-dimensional spaces, and some dimensions, such as velocities, are not suitable for estimating the accessibility values. Therefore, we should only do clustering in a subspace with feasible dimensions. Also, since the clustering results correspond to the initial states for learning, the subspace must include the necessary dimensions for initialization.

The second principle is about the reward function and the target state. In fall recovery, the target state can be defined as the standing pose. In other tasks such as backflipping, the target state can refer to a good starting pose that can get the maximum episode reward in the future.

The third principle is about the estimation of accessibility values. In fall recovery, we apply the response time of PD control. However, such heuristic estimation can only work for static poses, and there can be errors in some cases, e.g., when large torques make the robot fly. Also, more complicated and high-level controllers can be necessary for other scenarios. In such cases, a trade-off between complexity and estimation accuracy needs to be considered.

III. IMPLEMENTATION AND RESULTS

A. Sampling Static Poses

In the PyBullet environment, we randomly initialized the Bittle robot with roll angle $\phi \sim \text{U}(-\pi, \pi)$, pitch angle $\theta \sim \text{U}(-\frac{\pi}{2}, \frac{\pi}{2})$, yaw angle $\psi = 0$, and joint positions $p \sim \text{U}(-\frac{5}{6}\pi, \frac{5}{6}\pi)$. Self-collision cases were abandoned.

The robot was dropped from 0.35 m above the ground. If the robot was stationary within 2 seconds (with negligible velocity, angular velocity, and distance to the ground), we recorded the final joint positions, the final roll angle, the final pitch angle, and the body height. We assume the ground to be flat for sampling.

With 12× multiprocessing, we sampled 2.4k static poses within an hour on an ordinary desktop machine.

B. Estimating Accessibility Values

To estimate the accessibility from static pose A to static pose B, we initialized the robot with static pose A. Then we sent a command to the PD controllers with the joint positions of B as the target positions. If the robot entered static equilibrium within 3 seconds, we checked whether the state of robot was close to the state of B. If these two states were close enough, we recorded the time cost t and the estimated accessibility from A to B was e^{-t}. Otherwise, we set the accessibility from A to B to be 10^{-8} instead of zero because all the sampled static poses are assumed to be accessible.

We randomly selected 1k samples from the sampled static poses. With 12× multiprocessing, we obtained the 1M accessibility values for the 1k×1k accessibility matrix within 20 hours on an ordinary desktop machine.

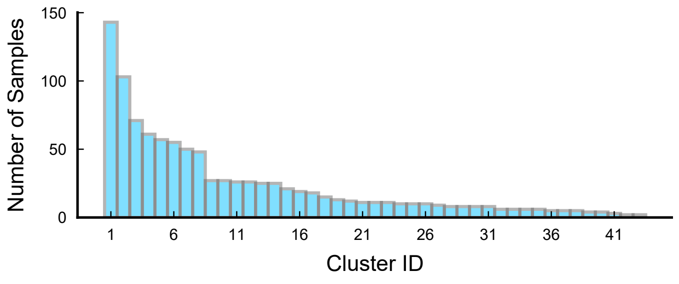

Fig. 7. Number of samples within each cluster when there are $k = 43$ clusters. The clusters are sorted by the number of samples assigned to them.

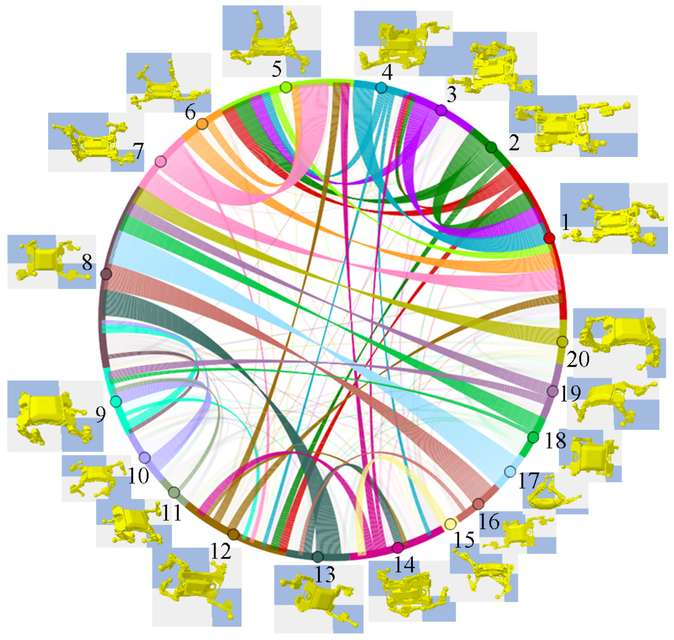

Fig. 8. Visualization of the inter-cluster accessibility of top-20 clusters. Inter-cluster accessibility values above 0.15 are highlighted, and those values below 0.05 are omitted here for clarity.

C. Clustering

We applied the proposed K-Access algorithm to the 1k$\times$1k accessibility matrix obtained in III-B. The α value for the index is 1. To determine the number of clusters k, we tried different k values and obtained the maximum index value when $k = 43$. The number of samples in each of the 43 clusters is shown in Fig. 7, indicating that the static poses of the robot are subjected to a long-tail distribution.

Figure 8 visualizes the inter-cluster accessibility of top-20 clusters via chord diagram, which can also contribute to pose taxonomy analysis [32] [33]. Different clusters correspond to different contact cases, and the inter-cluster accessibility corresponds to the difficulty of transitions.

D. Deep Reinforcement Learning

We applied six kinds of initial state distributions:

1) Centroids of the obtained 43 clusters by K-Access (abbreviated to KA);
2) Centroids of the obtained 33 clusters by K-Means++ based on the generalized Dunn's index $v43$ [34] (abbreviated to KM);

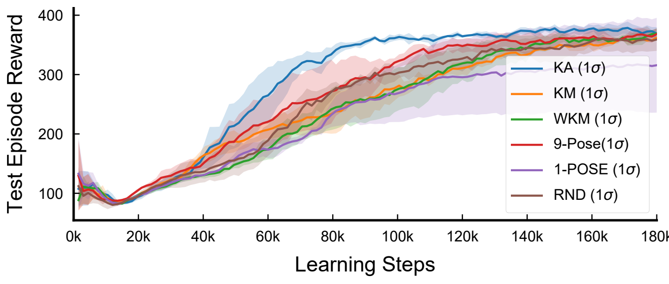

Fig. 9. Learning curves of fall recovery for different initial state distributions. The proposed method shows the highest data efficiency. There are 300 steps per episode, the discount factor is 0.987, the target smoothing coefficient is 0.001, and the learning rate is 3e-4. Averaged over 3 random seeds, with ± 1 SD. in shadow.

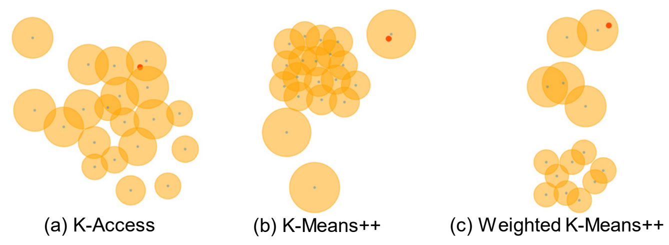

Fig. 10. Visualization of the obtained clusters for overlapping and coverage. The red points are the target standing pose. The blue points are the centroids of top 20 clusters for (a)-(b), and all of the 14 clusters for (c). The positions of the centroids follow a spring layout based on the inter-cluster accessibility values. The average accessibility values from the centroids to their neighbors, representing the expected burden of exploring the centroids, determine the radii of the circles. The K-Access centroids generate better initial states according to Fig. 4.

3) Centroids of the obtained 14 clusters by weighted K-Means++ based on $v43$ (abbreviated to WKM, gravity vector weighted by 2);
4) Nine initial poses applied in [4] (abbreviated to 9-Pose);
5) One lying pose (abbreviated to 1-Pose);
6) Random static poses (abbreviated to RND).

We demonstrate the proposed method can greatly improve the data efficiency, based on the learning curves using the same test samples shown in Fig. 9, which shows consistent results with Fig. 1. The centroids of KA, KM, and WKM are also visualized in Fig. 10 to validate our hypothesis in II.

Since the learning from different initial states can also be considered as different sub-tasks of varying difficulty, we also tried to combine the distributions with Teacher-Student Curriculum Learning (TSCL) [35]. The learning curves on the same test samples are shown in Fig. 11, and the TSCL can improve the efficiency under most of the random seeds.

For robustness, agents of the best seeds were tested on another 500 static poses. There are 75 steps (3 seconds) per episode during the test, and the criterion of success is that the reward at 3 s is larger than 1.2. The performance scores are presented in Table II. It can be seen that the proposed method can be used to learn robust fall recovery policies with 25% fewer steps than other distributions. Test runs are shown in the video attachment. Snapshots are in Fig. 13(a).

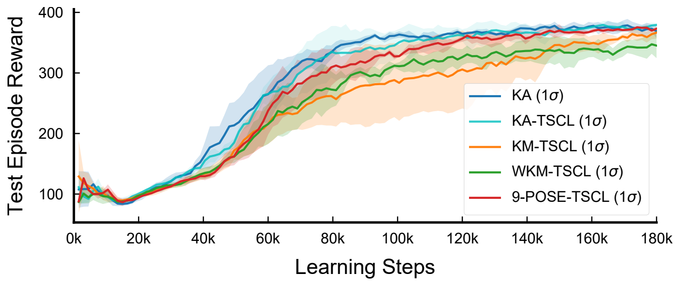

Fig. 11. Learning curves of fall recovery for different initial state distributions with TSCL. Simple POMDP Formulation applied, with Online algorithm ($\alpha = 0.2$, ε-greedy with $\varepsilon = 0.2$, abs). Hyperparameters of DRL not changed. Averaged over 3 random seeds, with ± 1 SD. in shadow.

TABLE II

PERFORMANCE ON THE TEST POSES

Initial States	Training Episodes	Episode Reward Mean	SD.	Success Rate in 3 s (%)
KA	**1200**	**81.93**	**11.84**	**99.4**
KM	1600	74.84	20.14	91.8
WKM	1600	79.04	18.20	94.4
9-Pose	1600	73.35	17.01	91.6
1-Pose	1600	73.09	17.75	92.6
RND	1600	79.97	17.32	94.6
KA-TSCL	1200	**84.70**	**13.38**	**98.6**
KM-TSCL	1200	75.55	16.97	95.2
WKM-TSCL	1200	77.11	15.65	95.4
9-Pose-TSCL	1200	77.01	18.07	93.8

E. Backflip Learning

We applied our proposed method to learn backflipping and the learning curves using the same test samples are in Fig. 12. Here we only clustered the static poses with roll angle less than 60 deg. Test runs are detailed in the paper's video, see snapshots in Fig. 13(b).

IV. Discussion

Although extra computation is required to estimate accessibility values before clustering, the proposed method can achieve high data efficiency for learning. Based on this learning-free metric, the centroids are only computed once, and they can boost the training process regardless of the design choices of DRL algorithms, hyperparameters, and reward functions. For a larger size of the accessibility matrix, one time-efficient way is to numerically fit the accessibility values with a small training batch of which the ground truth is obtained via simulation.

The K-Access algorithm performs better than the existing clustering methods because: 1) the direction of transitions is taken into consideration; 2) the neighbors in one cluster are all easy to explore from the centroid; 3) the number of clusters can be assigned and determined by the index value. The extension to backflipping also shows that, intermediate and unstable poses can be better explored with our method.

The visualization of inter-cluster accessibility also indicates that the patterns can be heuristic for learning fall recovery motions. Moreover, such patterns can also help design strategies for optimization-based methods [36].

For robustness over a large range of initial states, there are also other methods, such as region of attraction (RoA) expansion [37] [38]. In [37], the learning process is also

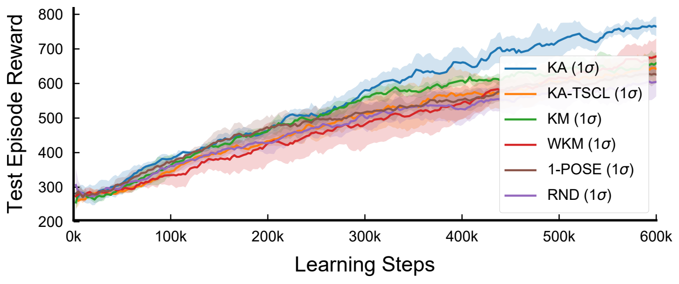

Fig. 12. Learning curves of backflipping for different initial state distributions. Averaged over 3 random seeds, with ± 1 SD. in shadow.

expedited by adaptive sampling, but the technique is based on the simplified representation of RoA that is difficult to implement in a high-dimensional nonlinear state space. It is also hard to combine the RoA expansion with the DRL process, since the DRL policy does not explicitly bridge the intermediate states as in [38]. However, the RoA expansion can be applied after the learning process to improve the robustness, and the robustness during the DRL process within finite steps can reduce the time cost and complexity of the subsequent RoA expansion.

V. Conclusion and Future Work

In this paper, we propose to automatically discover initial states for DRL of locomotion skills via the accessibility metric and the K-Access clustering algorithm. With the centroids of the obtained clusters as the initial states, the data efficiency of fall recovery learning can be greatly improved, and the robustness can be maintained. Our method can also be generalized to other tasks, such as backflipping.

Compared to the Euclidean distance metric, the proposed accessibility metric does not suffer from the non-orthogonality of the feature space and the undirected distances. Therefore, it can model the difficulty of transitions from one state to another much better.

Compared to random initialization, our method is more data efficient, as shown by our results in Fig. 9 and Fig. 12. Compared to the manually predefined initialization, our method is more robust, as benchmarked in Table II. TSCL does not improve the robustness since it focuses on the efficiency, and it does not work when all of the sub-tasks are hard in backflip learning.

Future work will focus on the general application of the clustering method. We will continue working on the possible extensions to other locomotion tasks that can benefit from the proposed method, and do hardware validation on other robot platforms, e.g., 12-DoF quadrupedal robots. We will also try other methods for better accessibility estimation, e.g., neural networks.

References

[1] S. Shamsuddin *et al.*, "Humanoid robot nao: Review of control and motion exploration," in *2011 IEEE international conference on Control System, Computing and Engineering*, 2011, pp. 511–516.

[2] I. Mordatch *et al.*, "Discovery of complex behaviors through contact-invariant optimization," *ACM Transactions on Graphics (TOG)*, vol. 31, no. 4, pp. 1–8, 2012.

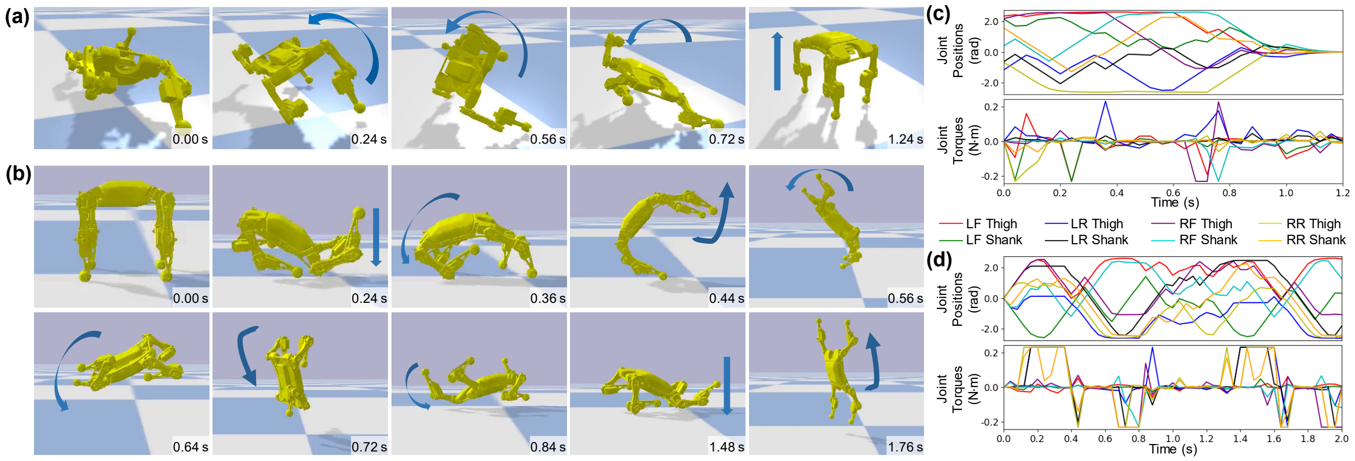

Fig. 13. Snapshots of (a) fall recovery and (b) continuous backflips. (c) shows the joint positions and torques for the case of fall recovery in (a), and (d) shows those for the case of backflipping in (b).

[3] O. Melon *et al.*, "Receding-horizon perceptive trajectory optimization for dynamic legged locomotion with learned initialization," in *Proceedings of the IEEE International Conference on Robotics and Automation (ICRA)*, 2021.

[4] C. Yang *et al.*, "Multi-expert learning of adaptive legged locomotion," *Science Robotics*, vol. 5, no. 49, 2020.

[5] X. B. Peng *et al.*, "Deepmimic: Example-guided deep reinforcement learning of physics-based character skills," *ACM Transactions on Graphics (TOG)*, vol. 37, no. 4, pp. 1–14, 2018.

[6] D. Reda *et al.*, "Learning to locomote: Understanding how environment design matters for deep reinforcement learning," in *Motion, Interaction and Games*, 2020, pp. 1–10.

[7] J. Yue, "Learning locomotion for legged robots based on reinforcement learning: A survey," in *2020 International Conference on Electrical Engineering and Control Technologies (CEECT)*, 2020, pp. 1–7.

[8] J. Hwangbo *et al.*, "Learning agile and dynamic motor skills for legged robots," *Science Robotics*, vol. 4, no. 26, 2019.

[9] M. Neunert *et al.*, "Whole-body nonlinear model predictive control through contacts for quadrupeds," *IEEE Robotics and Automation Letters*, vol. 3, no. 3, pp. 1458–1465, 2018.

[10] J. Lafaye *et al.*, "Model predictive control for tilt recovery of an omnidirectional wheeled humanoid robot," in *2015 IEEE international conference on robotics and automation (ICRA)*, 2015, pp. 5134–5139.

[11] I. Chatzinikolaidis *et al.*, "Contact-implicit trajectory optimization using an analytically solvable contact model for locomotion on variable ground," *IEEE Robotics and Automation Letters*, vol. 5, no. 4, pp. 6357–6364, 2020.

[12] J. Wang *et al.*, "Whole-body trajectory optimization for humanoid falling," in *2012 American Control Conference (ACC)*, 2012, pp. 4837–4842.

[13] K. Yuan *et al.*, "Bayesian optimization for whole-body control of high-degree-of-freedom robots through reduction of dimensionality," *IEEE Robotics and Automation Letters*, vol. 4, no. 3, pp. 2268–2275, 2019.

[14] J. Schulman *et al.*, "Proximal policy optimization algorithms," *arXiv preprint arXiv:1707.06347*, 2017.

[15] T. Haarnoja *et al.*, "Soft actor-critic algorithms and applications," *arXiv preprint arXiv:1812.05905*, 2018.

[16] N. Rudin *et al.*, "Learning to walk in minutes using massively parallel deep reinforcement learning," in *5th Annual Conference on Robot Learning*, 2021.

[17] X. Xu *et al.*, "A clustering-based graph laplacian framework for value function approximation in reinforcement learning," *IEEE Transactions on Cybernetics*, vol. 44, no. 12, pp. 2613–2625, 2014.

[18] J. MacQueen *et al.*, "Some methods for classification and analysis of multivariate observations," in *Proceedings of the fifth Berkeley symposium on mathematical statistics and probability*, vol. 1, no. 14. Oakland, CA, USA, 1967, pp. 281–297.

[19] M. Ester *et al.*, "A density-based algorithm for discovering clusters in large spatial databases with noise," in *Proceedings of the Second International Conference on Knowledge Discovery and Data Mining*, ser. KDD'96. AAAI Press, 1996, p. 226–231.

[20] F. D. Malliaros and M. Vazirgiannis, "Clustering and community detection in directed networks: A survey," *Physics reports*, vol. 533, no. 4, pp. 95–142, 2013.

[21] M. Bharatheesha *et al.*, "Distance metric approximation for state-space rrts using supervised learning," in *2014 IEEE/RSJ International Conference on Intelligent Robots and Systems*, 2014, pp. 252–257.

[22] S. M. LaValle *et al.*, "Rapidly-exploring random trees: A new tool for path planning," Computer Science Department, Iowa State University, Tech. Rep., 1998.

[23] M. E. Taylor *et al.*, "Metric learning for reinforcement learning agents," in *The 10th International Conference on Autonomous Agents and Multiagent Systems-Volume 2*, 2011, pp. 777–784.

[24] N. Dugué and A. Perez, "Directed louvain: maximizing modularity in directed networks," Ph.D. dissertation, Université d'Orléans, 2015.

[25] L. Bohlin *et al.*, "Community detection and visualization of networks with the map equation framework," in *Measuring scholarly impact*. Springer, 2014, pp. 3–34.

[26] D. Gleich, "Hierarchical directed spectral graph partitioning," *Information Networks*, vol. 443, 2006.

[27] Y. Kim *et al.*, "Finding communities in directed networks," *Physical Review E*, vol. 81, no. 1, p. 016103, 2010.

[28] D. Arthur and S. Vassilvitskii, "k-means++: The advantages of careful seeding," Stanford, Tech. Rep., 2006.

[29] X. B. Peng and M. van de Panne, "Learning locomotion skills using deeprl: Does the choice of action space matter?" in *Proceedings of the ACM SIGGRAPH/Eurographics Symposium on Computer Animation*, 2017, pp. 1–13.

[30] Petoi. (2021) Bittle robot. [Online]. Available: https://www.kickstarter.com/projects/petoi/bittle

[31] E. Coumans and Y. Bai, "Pybullet, a python module for physics simulation for games, robotics and machine learning," http://pybullet.org, 2016–2021.

[32] J. Borras and T. Asfour, "A whole-body pose taxonomy for loco-manipulation tasks," in *2015 IEEE/RSJ International Conference on Intelligent Robots and Systems (IROS)*, 2015, pp. 1578–1585.

[33] J. Borràs *et al.*, "A whole-body support pose taxonomy for multi-contact humanoid robot motions," *Science Robotics*, vol. 2, no. 13, 2017.

[34] J. C. Bezdek and N. R. Pal, "Cluster validation with generalized dunn's indices," in *Proceedings 1995 second New Zealand international two-stream conference on artificial neural networks and expert systems*, 1995, pp. 190–193.

[35] T. Matiisen *et al.*, "Teacher–student curriculum learning," *IEEE transactions on neural networks and learning systems*, vol. 31, no. 9, pp. 3732–3740, 2019.

[36] J. A. Castano *et al.*, "Design a fall recovery strategy for a wheel-legged quadruped robot using stability feature space," in *IEEE International Conference on Robotics and Biomimetics*, 2019, pp. 41–46.

[37] V. C. Kumar *et al.*, "Improving model-based balance controllers using reinforcement learning and adaptive sampling," in *2018 IEEE International Conference on Robotics and Automation (ICRA)*, 2018, pp. 7541–7547.

[38] M. A. Borno *et al.*, "Domain of attraction expansion for physics-based character control," *ACM Transactions on Graphics (TOG)*, vol. 36, no. 2, pp. 1–11, 2017.